Revista Brasileira de Aplicações de Vácuo, Vol. 11, n. 2, 1992.

BOOTSTRAP CURRENT FOR SMALL ASPECT RATIO TOKAMAK EQUILIBRIA

P.H. Sakanaka and D.L.G. Andreatta

Instituto de Física,
Universidade Estadual de Campinas
C.P. 6165 - 13081 Campinas, SP, Brasil

S. Tokuda

Japan Atomic Energy Research Institute
Naka Establishment, Tokai-mura, Ibaraki, Japan

ABSTRACT:

We present equilibrium features of the very small aspect ratio tokamak, TBR-2E, with the aspect ratio of 1.6, which is being designed in Brazil - a joint project with the participation of the University of São Paulo, the State University of Campinas, and the National Institute for Space Research.

The equilibria have been studied by using the SELENE-J code developed at JAERI, Japan, by Tokuda et al. We have concentrated our study on the determination of the stability limit by using the critical pressure criterium for ballooning stability and Mercier criterium for other MHD modes. The β-limit values were calculated for the case of the non-inductive current and found that its maximum lies at elongation of 1.7. Increasing the triangularity, the β-limit values increase, but the maximum continues to stay at the same value of elongation.

We have also studied the effect of the neo classical transport properties by changing the plasma temperature (or β values). In particular, we have studied the trapped particles and bootstrap current. We have found that at temperatures as low as 600 eV the transport is already in banana regime and that the bootstrap current may account for a significant part of the total plasma current.

1. INTRODUCTION

Triggered by Troyon scaling |1|, there have been many studies of very small aspect ratio tokamaks |2, 3| which show that, from the stability point of view, as one lowers the aspect ratio the plasma beta value increases. There are also several proposals and projects for the construction of a very small aspect ratio tokamak |5, 4, 6, 7|.

A joint project, TBR-2E, has been proposed by three Institutions in Brazil: University of São Paulo (USP), State University of Campinas (UNICAMP), and National Institute of Space Research (INPE), with the cooperation of Oak Ridge National Laboratory, USA |8|.

The design values of TBR-2E is given in Table I, the expected plasma parameters are given in Table II and the main cotes for the project is shown in figure 1.

Major radius	R_0 = 0.39 m
Mirror radius	a = 0.25 m
Maximum elongation	b/a = 1.7
Toroidal field at R_0 = 0.50	B_ϕ = 0.63 T
Plasma current	I_p = 260 kA
Cylindrical safety factor	q_c = 4.5
Plasma pulse duration	τ_p = 100 ms

Table I : Main design values for TBR-2E

Maximum average density	$\langle n_e \rangle = 1.0 \times 10^{20}$ m^{-3}
Average electron temperature	T_e = 700 eV
One-turn loop voltage ($Z_{eff} = 2$)	V_{loop} = 2 V
Maximum β (Troyon)	β = 10 %

Table II : Expected plasma values for TBR-2E

In section 2 the physical model is briefly described. In section 3 we report studies of equilibrium stability limit (mercier and ballooning) using the equilibrium code, SELENE-J, developed by S. Tokuda et al |9|. In section 4 we present the study of the bootstrap current generated in TBR-2E tokamak as a function of plasma current.

2. PHYSICAL MODEL

By expressing the equilibrium magnetic field as

$$\vec{B} = \nabla\phi \times \nabla\psi + F\nabla\phi , \quad (1)$$

where $F = RB_t$ (B_t, toroidal magnetic field), the Grad-Shafranov equation is derived:

$$\Delta^*\psi = R\mu_0 J_\phi , \quad (2)$$

where ψ is the poloidal flux function and the operator

$$\Delta^* = \frac{\partial^2}{\partial R^2} + \frac{\partial^2}{\partial Z^2} - \frac{1}{R}\frac{\partial}{\partial R}$$

In equation (2) J_ϕ is the toroidal current density given by

$$RJ_\phi = -R^2\frac{dp}{d\psi} - \frac{1}{\mu_0}F\frac{dF}{d\psi} , \quad (3)$$

$$RJ_\phi = 0 , \quad (4)$$

with $p = p(\psi)$ being the equilibrium pressure profile. Equation (3) is for the region inside the plasma and equation (4) in vacuum.

The quantity $\frac{dF}{d\psi}$ can be expressed in terms of the flux surface averaged parallel current density, $\langle \vec{J}.\vec{B} \rangle$

$$F\frac{dF}{d\psi} = -\mu_0 \left[\frac{F^2}{\langle B^2 \rangle}\frac{dp}{d\psi} + F\frac{\langle \vec{J}.\vec{B} \rangle}{\langle B^2 \rangle} \right] . \quad (5)$$

The surface averaged parallel current, $\langle \vec{J}.\vec{B} \rangle$, in equation (5) obeys the generalized Ohm's law |10, 11|.

$$\langle \vec{J}.\vec{B} \rangle = \langle \vec{J}.\vec{B} \rangle_{OHM} + \langle \vec{J}.\vec{B} \rangle_{BS} + \langle \vec{J}.\vec{B} \rangle_{NOHM} , \quad (6)$$

where $\langle \vec{J}.\vec{B} \rangle_{OHM}$ is the ohmic current, $\langle \vec{J}.\vec{B} \rangle_{BS}$ the bootstrap current and $\langle \vec{J}.\vec{B} \rangle_{NOHM}$ the non-ohmic current driven by external sources, such as, NBI and RF-wave. The ohmic and the bootstrap currents are expressed as

$$\langle \vec{J}.\vec{B} \rangle_{OHM} = \sigma_{NC}\langle \vec{E}.\vec{B} \rangle = \frac{n_e e^2 \tau_{ee}}{m_e}\Lambda_{NC}\langle \vec{E}.\vec{B} \rangle , \quad (7)$$

$$\langle \vec{J}.\vec{B} \rangle_{BS} = -F_{p_e}(L^e_{31}A_{p_e} + L^e_{32}A_{T_e}) - F_{p_i}(L^i_{31}A_{p_i} + L^i_{32}A_{T_i}) \quad (8)$$

where

$$A_{p_e} = \frac{d\,\ell n p_e}{d\psi} , \quad A_{T_e} = \frac{d\,\ell n T_e}{d\psi} ,$$

$$A_{p_i} = \frac{d\,\ell n p_i}{d\psi} , \quad A_{T_i} = \frac{d\,\ell n T_i}{d\psi} \quad (9)$$

and τ_{aa} is the Braginskii Coulomb collision time defined in |10|. The coefficients Λ_{NC}, L^e_{31}, L^e_{32}, L^i_{31}, and L^i_{32} in equations (7) and (8) are computed by the method given in references |10, 11|. This method is valid for finite aspect ratio, arbitrary cross-section, all collisionality regime, and multiple ion-species plasma.

In this work the following assumptions are used:

- plasma is in a stationary state: $\langle \vec{E}.\vec{B} \rangle = \langle \vec{B}.\nabla\phi \rangle V_L/2\pi$, with V_L being the one-turn voltage.
- only one impurity ion (Carbon) is considered.
- thermodynamic forces of the impurity are neglected. Impurity effects enters in the neoclassical coefficients of electrons and main ions only through Coulomb collisions.

Equation 6 demonstrates that the equilibrium is determined by specifying the density and temperature profiles of the electron and ions with the appropriate boundary and constraint conditions. In this work the total toroidal current, I_p, is employed as the constraint condition:

$$I_p = I_{PS} + I_{OHM} + I_{BS} = \text{given} , \quad (10)$$

where

$$I_{PS} = -\frac{1}{2\pi}\int \frac{dp\langle B_p^2 \rangle}{d\psi\langle B^2 \rangle} dV ,$$

$$I_{OHM} = \frac{1}{2\pi}\frac{V_L}{2\pi}\int \sigma_{NC}\left\langle \frac{1}{R^2} \right\rangle \frac{\langle B_t \rangle}{\langle B^2 \rangle} dV ,$$

$$I_{BS} = \frac{1}{2\pi}\int \frac{\langle \vec{J}.\vec{B} \rangle_{BS}}{\langle B^2 \rangle} F\left\langle \frac{1}{R^2} \right\rangle dV .$$

Here I_{PS} is the diamagnetic current and the Pfirsch-Schlüter return current which flows to maintain charge neutrality conditions on each flux surface, I_{OHM} is the Ohmic current, and I_{BS} is the bootstrap current.

Solving equation (2) together with equations (5) and (6) iteratively, V_L (one turn voltage) is updated at each iteration such that equation (10) is satisfied, i.e., V_L can be regarded as the nonlinear eigenvalue.

The operator Δ^* is numerically inverted by using the double cyclic reduction method in the Cartesian coordinate (R, Z) with the semi-fixed boundary method |9, 12|.

3. LIMITING BETA VALUES FOR TBR-2E

To solve the set of equations (2, 3, 4 and 5), we start by giving a set of vertical field and elongation coil positions and the profiles of $n_e(\psi)$, $T_e(\psi)$, $T_i(\psi)$, $Z_{eff}(\psi)$, and $\langle \vec{J}.\vec{B} \rangle$ in a general form:

$$f(\psi) = (f_0 - f_a)\ (1 - \psi)^{\alpha(\psi)} + f_a, \quad (11)$$

$$a(\psi) = a_0 + (a_E - a_0)\psi m\ . \quad (12)$$

Besides that, we have taken other parameters of TBR-2E and have chosen the triangularity, δ, to be 0.3. By varying its elongation, κ, from 1.0 to 2.2 we have checked the β-limit, i.e., the maximum plasma β value before plasma becomes either ballooning or Mercier unstable. We have increased the plasma temperature to insure the increase of β.

Figures 2 through 9 show a typical run for this study. In particular, we have taken a non-inductive current profile which brings a safety factor profile with q_0 being near unity and moderate magnetic shear.

Figure 2 plots the $\langle \vec{J}.\vec{B} \rangle$ profile; figure 3 shows the pressure and the q profiles; figure 4 shows the pressure derivative and the critical ballooning pressure derivative. As the temperature is increased the critical ballooning pressure derivative (dashed line) are raised. When this curve goes above the pressure derivative at some points, the ballooning instability sets in. In particular, figure 4 is the limiting case when plasma has just become unstable. Figure 5 is the Mercier creterion (thick solid line) and the three different terms which the Mercier criterion is composed of: shear term (dotted line), well term (thin solid line), and the destabilizing term (dashed line). Figures 6 and 7 show the pressure, q, n_e, and T_e profiles in R-space. Figure 8 shows the current density term: non-inductive current (thin solid line), Pfirsch-Schlüter current (dashed), and the total current profile (thick solid). Figure 9 shows the contour plot of $\psi(R, Z)$-function.

As we increase the temperature the stable equilibrium configuration becomes either ballooning or Mercier unstable. We have plotted the β-limit versus the elongation, κ, in figure 10, for two values of the triangularity, $\delta = 0.1$ and $\delta = 0.3$. We see that the maximum β-limit lies about elongation of $\kappa = 1.7$, and the β-limit is larger for larger triangularity. For $\kappa = 1.7$ and $\delta = 0.3$ we have $\beta = 0.075$. This calculations is the most stringent β limit calculation. If we choose the critical ballooning pressure derivatives at every flux surface, this β limit might be larger.

4. BOOTSTRAP CURRENT AND NEOCLASSICAL COLLISIONALITY FOR TBR-2E

We have run equilibrium cases for TBR-2E taking a close look at the neoclassical collisionality parameter and the bootstrap current.

The ratio between the average fraction of trapped particles to that of circulating particles is given by

$$g_t = \frac{f_t}{f_c} \quad (13)$$

where

$$f_c = \frac{3 \langle B^2 \rangle}{4 (B_{max})^2} \int_0^1 \frac{\lambda d\lambda}{\langle \sqrt{1 - \lambda B/B_{max}} \rangle} \quad (14)$$

$$f_t = 1 - f_c\ . \quad (15)$$

Now the average transit frequency of the species a is defined by

$$\omega_{ta} = v_{Ta} \left(\frac{1}{\sqrt{g}B}\right) \simeq \frac{v_{\theta a}}{R_0 q} \quad (16)$$

where $\sqrt{g} = |(\nabla\psi \times \nabla\theta).\nabla\theta|^{-1}$, $v_{Ta} = \sqrt{2T_a/m_a}$, R_0 is the position of the magnetic axis, and q is the safety factor. The collisionality parameter ν^* is given by [12]

$$\nu^* = \frac{g_t}{2.92} \left(\frac{1}{\sqrt{g}B}\right) \frac{\langle B^2 \rangle}{\langle (\vec{B}.\nabla B/B)^2 \rangle}\ . \quad (17)$$

The three collisionality regimes for each species can be written.

Pfirsch-Schlüter regime: $1 << \frac{1}{\omega_{ta}\tau_{aa}}$,

Plateau regime: $\frac{1}{\nu^*} << \frac{1}{\omega_{ta}\tau_{aa}} << 1$,

Banana Regime: $\frac{1}{\omega_{ta}\tau_{aa}} << \frac{1}{\nu}$.

Now, when there are no trapped particles, neoclassical conductivity σ_{NC} reduces to the classical Spitzer conductivity $\sigma_{Spitzer}$.

Figure 11 shows the partition between trapped and circulating particles for the case of $T_e = 600$ eV. The trapped particles occupy between 60% to 80% of the total particles, which is very high.

In figure 12 we see the ratio between the neo-classical and Spitzer conductivy (1), which reaches about the value 0.4, and the collisionality curve (2), which means that when it is above 1 it is in banana regime. As one can see, the major part of electrons is in banana regime.

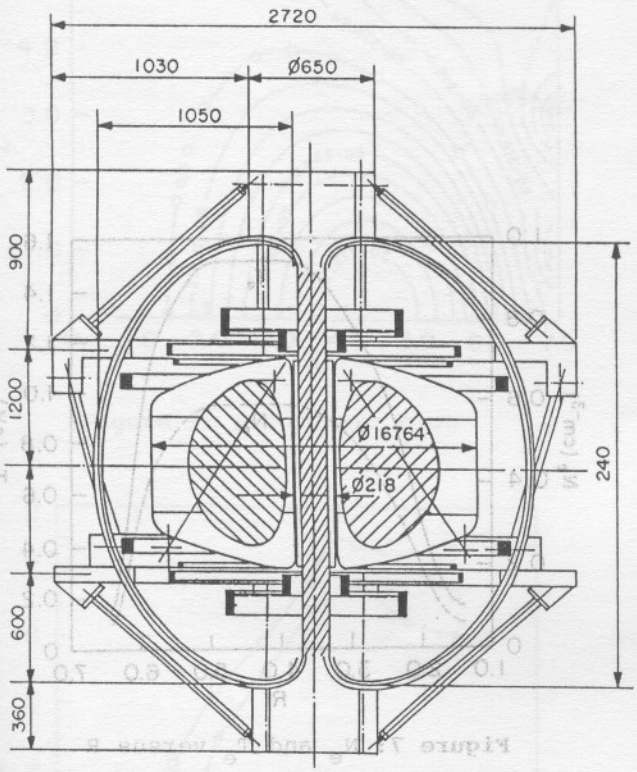

Figure 1: Main cotes (in millimeters) for the design of TBR-2E

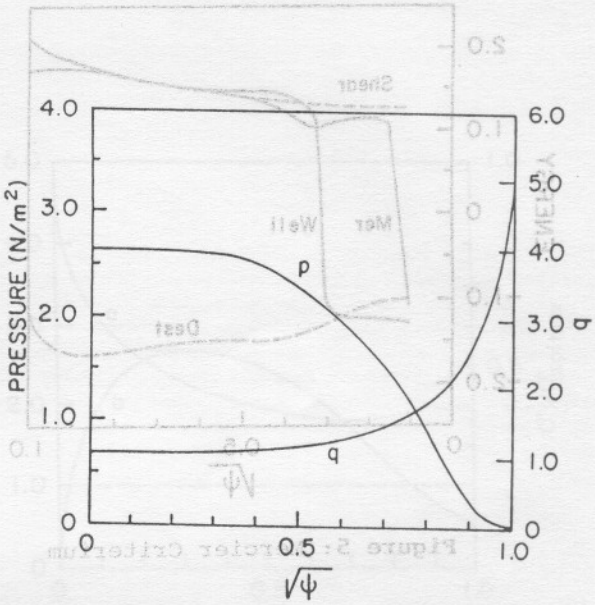

Figure 3: p and q versus $\sqrt{\psi}$

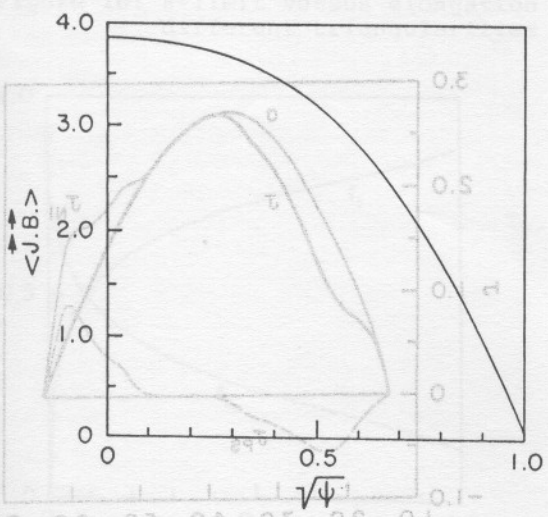

Figure 2: $\langle \vec{J}.\vec{B} \rangle$ versus $\sqrt{\psi}$

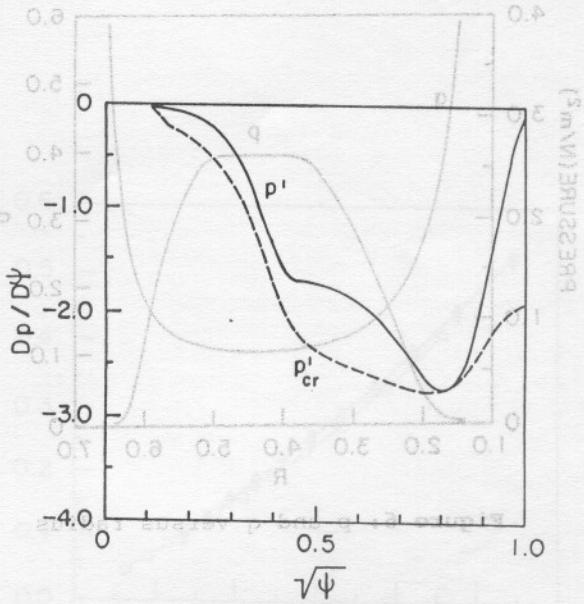

Figure 4: p' and P'_{cr} versus $\sqrt{\psi}$

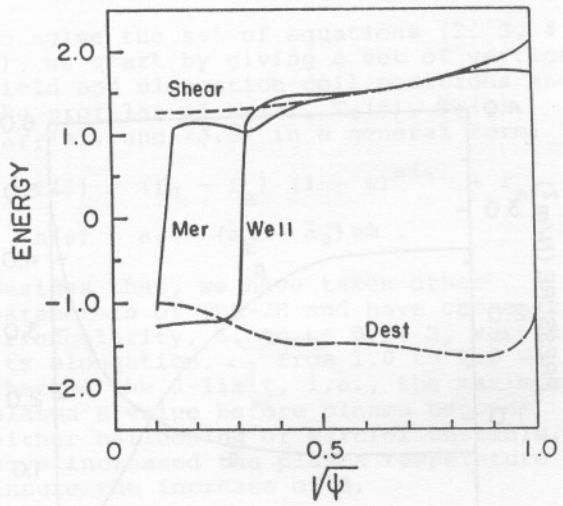

Figure 5: Mercier Criterium

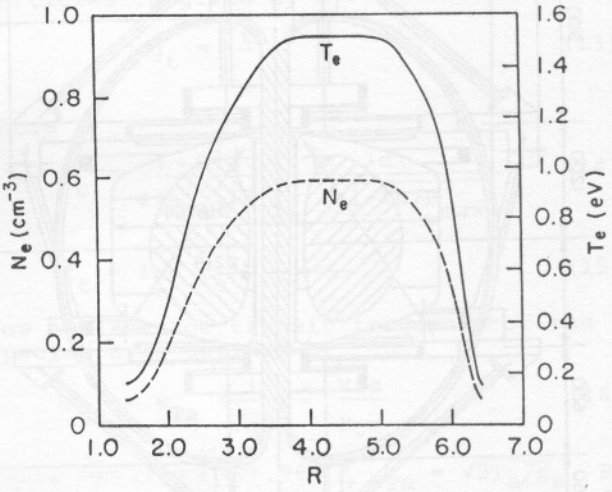

Figure 7: N_e and T_e versus R

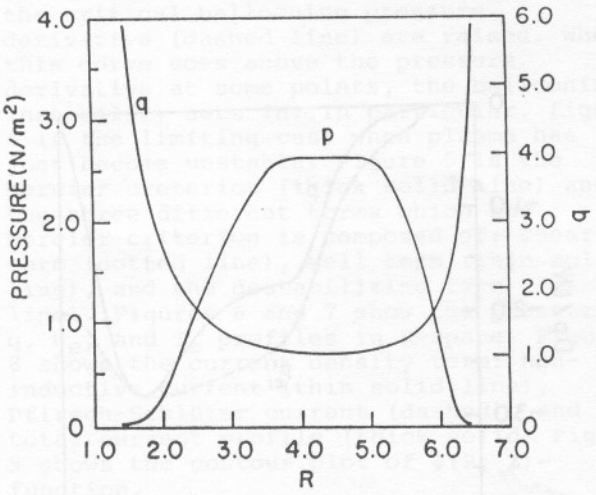

Figure 6: p and q versus radius

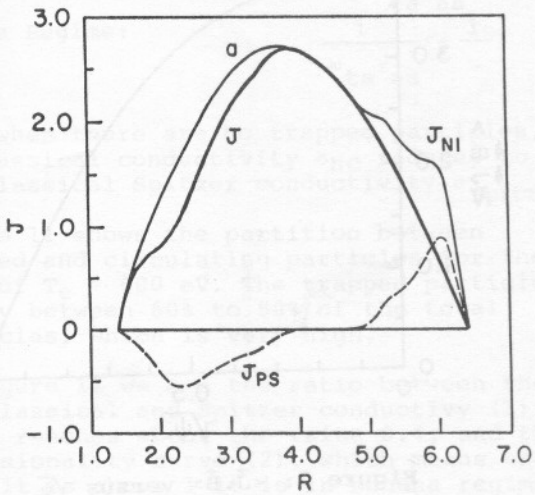

Figure 8: Current densities versus radius

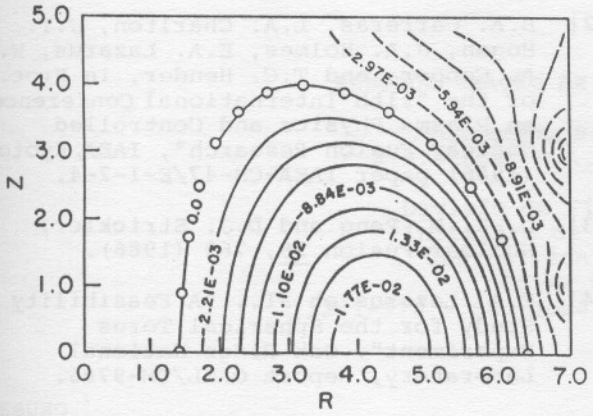

Figure 9: ψ contours plot

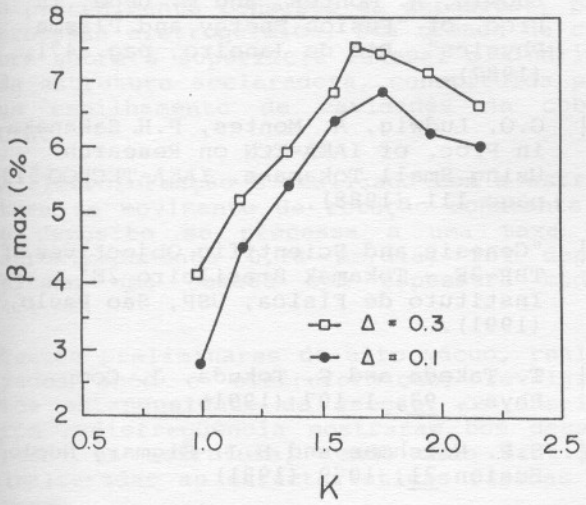

Figure 10: β-limit versus elongation for different triangularities

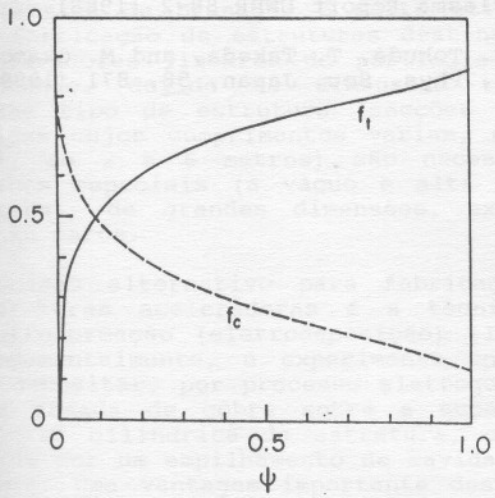

Figure 11: Trapped and circulating particle ratio versus ψ.

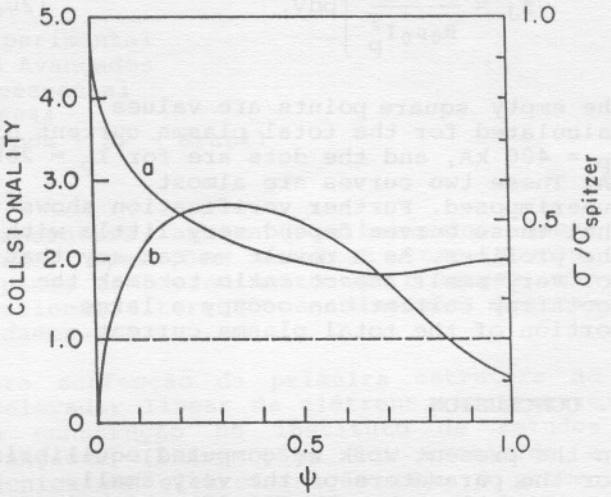

Figure 12: Ratio between Neo-classical and Spitzer conductivity (curve a) and collisionality (curve b) versus ψ.

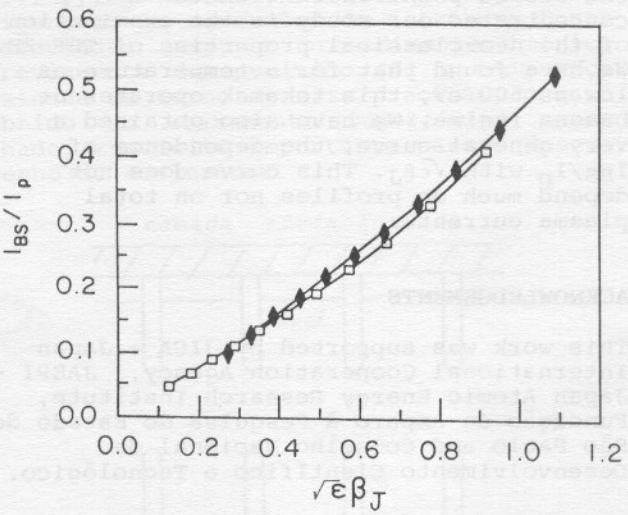

Figure 13: I_{BS}/I_p versus $\sqrt{\varepsilon}\beta_J$ and different I_p.

Figure 13 shows the dependence of the ratio I_{BS}/I_p with $\sqrt{\varepsilon}\beta_J$, where I_{BS} is the bootstrap current, I_p is the total plasma current, $\varepsilon = a/R_0$ is the inverse aspect ratio, and the current-beta given by

$$\beta_J = \frac{1}{R_0 \mu_0 I_p^2} \int p dV. \qquad (20)$$

The empty square points are values calculated for the total plasma current of I_p = 400 kA, and the dots are for I_p = 260 kA. These two curves are almost superimposed. Further verification shows that these curves depend very little with the profiles. As a result we can say that for very small aspect ratio tokamak the bootstrap current can occupy a large portion of the total plasma current.

5. CONCLUSION

In the present work we computed equilibria for the parameters of the very small aspect ratio tokamak, TBR-2E, which is being designed in Brasil. We have paid close attention, first, to the β-limit by varying the elongation with fixed triangularity. We have found that the maximum beta is obtained for values of beta near the natural elongation of the machine, particularly for the aspect ratio of 1.6 the maximum lies around κ = 1.7. Two values of triangularity we examined, δ = 0.1 and 0.3. For larger δ we have larger beta maximum.

The second point which we have concentrated our study is the examination of the neo-classical properties of TBR-2E. We have found that for a temperature as low as 600 eV, this tokamak operates at banana regime. We have also obtained a very general curve, the dependence of I_{BS}/I_p with $\sqrt{\varepsilon}\beta_J$. This curve does not depend much on profiles nor on total plasma current.

ACKNOWLEDGEMENTS

This work was supported by JICA - Japan International Cooperation Agency, JAERI - Japan Atomic Energy Research Institute, Fundação de Amparo à Pesquisa do Estado de São Paulo and Conselho Nacional de Desenvolvimento Científico e Tecnológico.

REFERENCES

|1| F. Troyon. R. Gruber, H. Saurenman, S. Semenzato, and S. Succi, Plasma Phys. and Controlled Fusion 26, 209 (1974).

|2| B.A. Carreras, L.A. Charlton, J.T. Hogan, J.A. Holmes, E.A. Lazarus, W. A. Cooper, and T.C. Hender, in Proc. of the "11th International Conference on Plasma Physics and Controlled Nuclear Fusion Research", IAEA, Kyoto (1986) paper IAEA-CN-47/E-1-2-4.

|3| U.-K. M. Peng and D.J. Strickler, Nuclear Fusion 26, 769 (1986).

|4| E.A. Lazarus et al., "A Feasibility Study for the Spherical Torus Experiment". Oak Ridge National Laboratory, Report ORNL/TM-9786.

|5| T. Todd et al. "START Project", Culham.

|6| R.M.O. Galvão, L.C.S. Goes, G.O. Ludwig, A. Montes, and M. Ueda, in Proc. of "Fusion Energy and Plasma Physics", Rio de Janeiro, pag. 471, (1987).

|7| G.O. Ludwig, A. Montes, P.H. Sakanaka in Proc. of IAEA-TCN on Research Using Small Tokamaks. IAEA-TECDOC-519 page 111 (1988).

|8| "Genesis and Scientific Objectives of TBR-2E - Tokamak Brasileiro 2E", Instituto de Física, USP, São Paulo, (1991).

|9| T. Takeda and S. Tokuda, J. Comp. Phys., 93, 1-107 (1991).

|10| S.P. Hirshman and D.J. Sigmar, Nucl. Fusion 21, 1079 (1981).

|11| Y.B. Kim, "Moment Approach to Neoclassical Flows, Currents and Transport in Auxiliary Heated Tokamaks", University of Wisconsin Plasma Report UWPR 88-2 (1988).

|12| S. Tokuda, T. Takeda, and M. Okamoto, J. Phys. Soc. Japan, 58, 871 (1989).